Resilience by diversity: Large intraspecific differences in climate change responses of an Arctic diatom

Klara K. E. Wolf [ID],* Clara J. M. Hoppe, Björn Rost
Marine Biogeosciences, Alfred Wegener Institute – Helmholtz Centre for Polar and Marine Research, Bremerhaven, Germany

Abstract

The potential for adaptation of phytoplankton to future climate is often extrapolated based on single strain responses of a representative species, ignoring variability within and between species. The aim of this study was to approximate the range of strain-specific reaction patterns within an Arctic diatom population, which selection can act upon. In a laboratory experiment, we first incubated natural communities from an Arctic fjord under present and future conditions. In a second step, single strains of the diatom *Thalassiosira hyalina* were isolated from these selection environments and exposed to a matrix of temperature (3°C and 6°C) and pCO$_2$ levels (180 μatm, 370 μatm, 1000 μatm, 1400 μatm) to establish reaction norms for growth, production rates, and elemental quotas. The results revealed interactive effects of temperature and pCO$_2$ as well as wide tolerance ranges. Between strains, however, sensitivities and optima differed greatly. These strain-specific responses corresponded well with their respective selection environments of the previous community incubation. We therefore hypothesize that intraspecific variability and the selection between coexisting strains may pose an underestimated source of species' plasticity. Thus, adaptation of phytoplankton assemblages may also occur by selection *within* rather than only *between* species, and species-wide inferences from single strain experiments should be treated with caution.

In times of growing concern about the effects of climate change, the Arctic Ocean and its ecosystems are of special interest. Arctic ocean warming and acidification are much stronger than on global average (AMAP 2013; IPCC 2013) and can be viewed as an early indicator to what may occur elsewhere in the decades to come. The winter of 2015/2016 with high temperatures and another all-time-low of sea ice (Cullather et al. 2016) may provide a taste of the future Arctic, with ice-free summers predicted within the next 30 yr (Wadhams 2012). Seawater pH is expected to drop by up to 0.4 units under the anticipated scenario of 1000 μatm pCO$_2$ in the atmosphere (AMAP 2013). The ramifications of these changing conditions on the northern polar ecosystems are still difficult to monitor and even harder to predict. It is therefore crucial to gain a better understanding of how primary producers at the base of the food web will respond to the alteration of these environmental drivers. The majority

of photosynthesis in oceanic environments is sustained by phytoplankton, with diatoms accounting for 40% of global primary production (Sarthou et al. 2005) and being especially dominant in polar regions (Poulin et al. 2011). Unicellular primary producers are not only the very base of the aquatic food-web but they also substantially influence global biogeochemical cycles by CO$_2$-fixation and carbon export as well as by oxygen production (Field et al. 1998).

Although the effects of warming and ocean acidification have been increasingly studied over the last decade, investigations on the responses of diatoms toward the predicted changes often yielded contradictive results. In laboratory studies, conceptual and methodological differences may partly explain such apparent disagreements. For instance, next to differences in the tested levels of CO$_2$ and temperature, other environmental drivers (e.g., light or nutrient supply) are often not comparable between studies. Such boundary conditions, however, have been found to strongly modulate the responses to warming and ocean acidification (e.g., Kranz et al. 2011; Gao and Campbell 2014). Many laboratory studies also use species and strains from different regions, or cultures that have been kept in artificial conditions for years or decades - timescales that are evolutionarily relevant for phytoplankton (Lakeman et al. 2009; Collins et al. 2013). Despite these uncertainties, some general

*Correspondence: klara.wolf@awi.de

patterns can be recognized: Moderate increases in temperature usually accelerate growth as well as primary production, following the Q10-law (e.g., Tjoelker et al. 2001; Hare et al. 2007; Gao et al. 2012). Responses toward rising CO_2 on diatoms have, however, been reported to vary strongly, ranging from growth rate inhibition to stimulation or an absence of response (e.g., Torstensson et al. 2011; Trimborn et al. 2013; Gao and Campbell 2014). In view of these findings, it is meanwhile recognized that impacts of one factor can only be understood in the context of others by designing multiple stressor experiments (Häder and Gao 2015; Hoppe et al. 2015) and that information on more than one representative of a species or functional group is required to make thorough predictions (Langer et al. 2009; Schaum et al. 2012).

Next to laboratory studies, manipulations of field assemblages have yielded important insights on how responses on the level of monoclonal cultures can be amplified or buffered on the ecosystem level (e.g., Schulz et al. 2013; Tatters et al. 2013; Coello-Camba et al. 2014; Holding et al. 2015). Processes that determine the sensitivity or resilience of phytoplankton assemblages to changing conditions can take place on different scales. The first level of a response is the phenotypic plasticity of a single individual, which can be surveyed by investigating the tolerance range or reaction norm of a single strain to a range of treatments after a phase of acclimation (Collins et al. 2013; Sett et al. 2014). A second level lies in the intraspecific diversity, i.e., the sum of tolerance ranges of individuals of the same species. Hence, it describes the functional diversity within a species or population. This integrated phenotypic plasticity of a species is an often overlooked but important basis for natural selection to act upon, since direct competition does not take place between taxonomic groups but between individuals (Collins et al. 2013; Rynearson and Menden-Deuer 2016). The third level of response to environmental change concerns species shifts within the community, which have often been observed in community incubations as well as long-term field monitoring (Tortell et al. 2008; Hoppe et al. 2013; Nöthig et al. 2015). Changes in species composition may be the most conspicuous consequence of a changing environment and can have large impacts on other trophic levels and elemental cycles. All these levels must be considered when discussing the resilience of a species or an ecosystem because a failure to cope with changing conditions on one level will lead to a shift in the next. At the same time, large plasticity on a lower level may "buffer" effects on a higher one.

A high intraspecific diversity of diatoms has been realized as far back as 1982, when Gallagher and co-workers found significant differences in the response of diatom strains and warned not to use "single clones to analyze the response of natural populations." This statement proved valid in later investigations on strain-specific differences in physiological responses as well (e.g., Brand 1989; Kremp et al. 2012; Pančić et al. 2015; Menden-Deuer and Kiørboe 2016; Sildever et al.
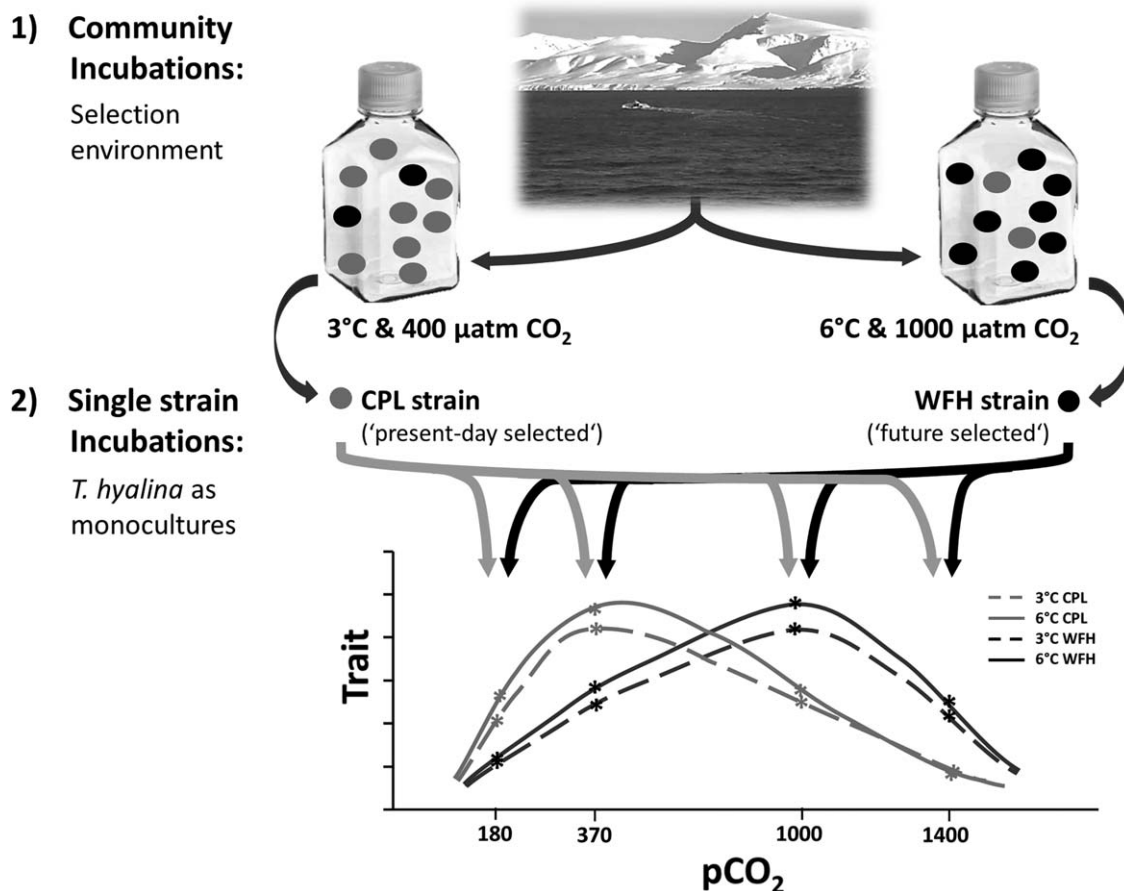
2016; Hattich et al. 2017). Even using advanced genetic tools nowadays, strain diversity is still troublesome to resolve and therefore not frequently measured. In all diatom populations examined so far, however, diversity was found to be impressively large, with consistent reports of 95–100% diversity among genotypes (Rynearson and Armbrust 2000; Evans et al. 2005; Casteleyn et al. 2009; Härnström et al. 2011). Even within a single diatom bloom, intraspecific diversity remains extremely high (Chen and Rynearson 2016; Sildever et al. 2016). For Arctic phytoplankton species, to our knowledge there is only one record of genotypic (Tammilehto et al. 2016) and one of physiological diversity available (Pančić et al. 2015), which both found large intraspecific diversity.

In this study, we used an innovative two-step approach that combined manipulations on field assemblages and physiological measurements on single-strain isolates in order to address the plasticity on the individual as well as on the population level (Fig. 1). In a *first* step, we incubated a natural Arctic community in a multiple-stressor-experiment for two weeks, allowing it to adjust its physiology and composition. We then isolated single cells of *Thalassiosira hyalina*, which is a dominant Arctic diatom species (Hegseth et al. in press). In a *second* step, two of these isolated strains, taken from the most extreme treatments (resembling present and anticipated future conditions in the fjord, i.e., low temperature and pCO_2 and high temperature and pCO_2 respectively), were incubated as monoclonal cultures to test for their individual responses toward changes in CO_2 and temperature. With this sequential design, we intended to assess two important aspects of adaptation at the same time: On the one hand, individual phenotypic plasticity was investigated by describing optima and tolerance ranges in response to one parameter (four pCO_2 treatments) and in dependence of another (two temperatures). We thus also aimed at taking interactive effects into account. On the other hand, the experimental design comprises the potential to examine those strains at differing extremes of the phenotypic diversity range within the population. This is because our isolated strains were not chosen randomly from the natural population, but in a way that favored those that were best adapted to our treatments of interest.

Material and methods

Community incubation experiment and strain isolation

A natural Arctic phytoplankton assemblage was grown in an incubation experiment, applying combined CO_2, temperature, and light treatments. This initial phytoplankton assemblage was sampled from the Kongsfjorden (mid-fjord station KB3, 78°55′N, 11°56′E; Svalbard) in April 2014, by pumping seawater from a depth of 23 m into 4 L polycarbonate bottles using a monsoon pump (Mega-Thyphoon, Proactive Environmental Products, U.S.A.; flow rate approx. 4 L min^{-1}). Seawater for the initiation of the experiment

Fig. 1. Schematic diagram of the experimental setup of this study: 1) natural community incubations under present-day- (3°C, 400 μatm pCO$_2$, 30 μmol photons m^{-2} s^{-1}) and future-conditions (6°C, 1000 μatm pCO$_2$, 150 μmol photons m^{-2} s^{-1}) and subsequent isolation of single strains, 2) single strain incubations within a multiple stressor matrix of temperature and pCO$_2$ (in μatm) for the establishment of reaction norms.

was filtered through a 200 μm mesh to eliminate large grazers. For later dilutions of the incubations, seawater was taken at the same time and location, filtered through 0.2 μm filter cartridges (AcroPak 1500, PALL) and subsequently stored at 3°C in the dark until use.

The bottles were incubated in growth chambers of the Kingsbay AS Marine Laboratory (Svalbard) at 3 ± 1°C and 6 ± 1°C and irradiances of 30 ± 10 and 150 ± 10 μmol photons m^{-2} s^{-1} (Master TL-D 18W daylight lamps, Philips, adjusted by neutral density screens). In accordance with the midnight sun in their natural environment during spring, we applied continuous light. To mimic different pCO$_2$ conditions, the incubation bottles were continuously aerated with air containing pCO$_2$ levels of 400 μatm and 1000 μatm, delivered through sterile 0.2 μm air-filters (Midisart 2000, Sartorius stedim). These gas mixtures were generated by a custom-built gas mixing system (*see* Hoppe et al. 2015). Experiments were run in triplicates and lasted between 10 and 13 d, depending on experimental treatment and respective community growth. In order to prevent significant changes in chemical conditions due to phytoplankton growth, incubations were

diluted with filtered seawater twice over the course of the experiment. Carbonate chemistry was monitored and treatment levels were found to vary by less than 0.03 pH units over time (Supporting Information Table 1).

To determine the taxonomic compositions, duplicate aliquots of 200 mL unfiltered seawater were preserved with glutaraldehyde (0.2% final concentration) or Lugols solution (1% final concentration). Samples were stored at 4°C in the dark until further analysis by inverted light microscopy (Axio Observer, Zeiss). Additionally, several dominant diatom species were identified according to taxonomic literature (Hasle and Syvertsen 1997) using scanning electron microscopy (SEM, Philips XL30). Biovolume was calculated after Hillebrand et al. (1999) and based on light microscopy measurements.

Single cells of the diatom *T. hyalina*, the dominating species in the final assemblages (see Supporting Information Table 2), were isolated manually under a light microscope or by dilution series, and the resulting stock cultures were maintained at 4°C. They originated from the final time point of the two most contrasting experimental conditions in the

community incubations, i.e., 3°C, 400 μatm pCO$_2$, 30 μmol photons m^{-2} s^{-1} (strain CPL = Cold Present-pCO$_2$ Low light) and 6°C, 1000 μatm pCO$_2$, 150 μmol photons m^{-2} s^{-1} (strain WFH = Warm Future-pCO$_2$ High-light). Mean cell diameter throughout the experiment was 15.5 ± 0.3 μm for the CPL strain and 17.8 ± 0.6 μm for the WFH strain. Cell sizes were determined by Coulter counter measurements and SEM observations. In spite of our efforts, a minute contamination by another substantially smaller *Thalassiosira* species was found in the CPL strain culture (possibly *Thalassiosira concaviuscula*). As *T. hyalina* dominated the biomass at any stage of the experiment ($> 99.9\%$), it did not affect the physiological analyses and interpretation. In addition to optical measures, genetic examination by means of rDNA sequencing (SSU, LSU, ITS) confirmed that both experimental strains belonged to the same species (to our knowledge, no sequences of *T. hyalina* are currently available).

Experimental conditions for single strain experiments

Cultures of the two strains were grown in 1 L glass bottles in semi-continuous dilute-batch cultures (200–10,000 cells mL^{-1}, diluted every 2–4 d). All sampling and dilutions were conducted under sterile conditions using a lamina flow hood. Cells were cultivated in 0.2 μm sterile-filtered Arctic seawater (collected in 2013 at N79° 53.589′ E10° 25.277′; salinity 32.7) enriched with macronutrients (NO$_3^-$, HPO$_4^{2-}$, SiO$_2$), vitamins and trace metals according to f/2 media (Guillard and Ryther 1962). Cells were grown under continuous light with 110 ± 10 μmol photons m^{-2} s^{-1} using daylight lamps (Biolux T8, 6500K, Osram, München, Germany). Irradiance was measured in filled culturing bottles using a 4π sensor (Walz, Effeltrich, Germany).

For the temperature treatments, target values of 3°C and 6°C were chosen to simulate the minimum and maximum temperatures cells are presently experiencing during spring and early summer blooming season in the Kongsfjord (Hegseth et al. in press). These temperatures also represent the current and expected future mean summer temperatures (Beszczynska-Möller et al. 2013). Experiments were performed in a temperature-controlled room of the Alfred Wegener Institute (Bremerhaven, Germany), with bottles immersed in water-filled aquaria for additional temperature stability (except for the 6°C treatment of WFH, which was conducted in a Rumed incubator (1301, Rubarth Apparate)). Continuous surveillance with a temperature logger (Almemo 2890, Ahlborn, Holzkirchen, Germany) ensured temperature stability at 3.3 ± 0.6°C and 5.9 ± 0.6°C.

Target pCO$_2$ was established by continuous aeration with a gas flow rate of $\sim$ 170 mL min^{-1}. The appropriately mixed air was delivered through sterile 0.2 μm air-filters (Midisart 2000, Sartorius stedim) by a custom-made gas mixing system (see above). Before inoculation and dilutions, seawater was equilibrated ($\geq$ 24 h) to the respective pCO$_2$ at treatment temperature. Prior to the experimental phase, cultures were

acclimated to treatment conditions for 4–7 d (> 6 generations). The responses of each strain were tested at a total of 8 treatments, i.e., low and high temperatures (3°C; 6°C) at four pCO$_2$ levels, representing present and future scenarios as well as extremes below and above that (180 μatm, 370 μatm, 1000 μatm, 1400 μatm). Each treatment was conducted in biological triplicates (except for CPL at 3°C and 1400 μatm where $n = 2$).

Carbonate chemistry measurements

Total alkalinity (TA) and dissolved inorganic carbon (DIC) samples of each replicate as well as of control bottles containing sterile medium were taken during the final sampling. TA samples were 0.7 μm-filtered (GF/F, Whatman, Maidstone, UK) and stored in 250 mL borosilicate bottles at 3°C until analysis. TA was determined by duplicate potentiometric titrations (Brewer et al. 1986) using a TitroLine alpha plus autosampler (Schott Instruments, Mainz, Germany). DIC samples were 0.2 μm-filtered (Cellulose-acetate syringe-filters, Sartorius stedim) and stored head-space free in 5 mL gastight borosilicate bottles at 3°C. DIC was measured colorimetrically in duplicates with a QuaAAtro autoanalyzer (Seal Analytical, Mequon, U.S.A.) after Stoll et al. (2001). Certified Reference Materials supplied by A. Dickson (Scripps Institution of Oceanography, U.S.A.) were used to correct for inaccuracies of TA and DIC measurements with a reproducibility of ± 16 μmol kg^{-1} ($n = 6$) and ± 9.7 μmol kg^{-1} ($n = 40$), respectively. Over the duration of the experiments, deviations in DIC of the incubations compared to abiotic controls were $< 5\%$ in all treatments. Stability of carbonate chemistry was ensured by daily measurements of pH (NBS scale) using a three-point calibrated potentiometric glass reference electrode cell (Aquatrode plus Pt1000, Metrohm, Herisau, Switzerland). Values were corrected for temperature variation and offsets in electrode performance using a TRIS-based certified reference standard (CRMs provided by Prof. A. Dickson, Scripps Institution of Oceanography, U.S.A., reproducibility ± 0.019 pH units, $n = 45$). Based on the TRIS buffer's assigned value, pH values were converted to total scale. Following Hoppe et al. (2012), calculations of the carbonate system (Table 1) were based on measurements of TA and pH, using the program CO$_2$ sys (Pierrot et al. 2006) with dissociation constants K1 and K2 by Mehrbach et al. (1973; refitted by Dickson and Millero 1987).

Growth, cellular composition and production rates

Specific growth rate constants μ (d^{-1}) were calculated by an exponential fit through measured cell numbers for each time point by the formula:

$$\mu = (\ln N_t - \ln N_0)/\Delta t$$

where μ refers to the growth rate constant, N_t to cell density at time t, N_0 to the initial cell density and Δt to the passed time (in days) since the start of the incubation. Cell densities (as cells mL^{-1}) were counted on a daily basis using a Coulter

Table 1. Parameters of the carbonate system for each treatment as mean $\pm$ standard deviation of biological replicates ($n = 3$) at the final incubation day. CO_2 partial pressure (pCO_2) was calculated from total alkalinity (TA) and pH_{total} at the respective temperature and a salinity of 32.5 using CO_2 SYS (Pierrot et al. 2006) with concentrations of 37 μmol kg^{-1} and 100 μmol kg^{-1} for phosphate and silicate, respectively.

Strain/treatment			pCO_2 [μatm]	pH_{total}	TA [μmol kg^{-1}]	DIC [μmol kg^{-1}]
CPL	3°C	180	205 ± 22	8.27 ± 0.01	2338 ± 7	2109 ± 22
		370	381 ± 12	8.06 ± 0.01	2332 ± 21	2192 ± 17
		1000	894 ± 36	7.72 ± 0.01	2363 ± 18	2337 ± 1
		1400	1308 ± 28	7.56 ± 0.0	2339 ± 24	2361 ± 3
CPL	6°C	180	185 ± 6	8.32 ± 0.01	2281 ± 46	2088 ± 29
		370	339 ± 10	8.10 ± 0.01	2294 ± 11	2195 ± 9
		1000	972 ± 22	7.69 ± 0.02	2324 ± 48	2290 ± 8
		1400	1445 ± 7	7.53 ± 0.0	2351 ± 12	2357 ± 4
WFH	3°C	180	166 ± 1	8.38 ± 0.0	2356 ± 5	2158 ± 48
		370	363 ± 29	8.07 ± 0.04	2273 ± 51	2214 ± 44
		1000	670 ± 66	7.82 ± 0.04	2264 ± 24	2262 ± 6
		1400	1391 ± 13	7.52 ± 0.04	2274 ± 24	2329 ± 38
WFH	6°C	180	168 ± 46	8.37 ± 0.11	2283 ± 44	1961 ± 91
		370	363 ± 65	8.08 ± 0.07	2337 ± 8	2130 ± 64
		1000	991 ± 103	7.69 ± 0.04	2351 ± 12	2338 ± 28
		1400	1351 ± 131	7.56 ± 0.04	2346 ± 11	2346 ± 36

CPL: present-day-selected strain; WFH: future-selected strain.

Multisizer III (Beckman-Coulter, Fullerton, U.S.A.), where *T. hyalina* cells were quantified within a size range of 13 μm and 21 μm.

For particulate organic carbon (POC) and nitrogen (PON), cells were filtered onto precombusted (15 h, 500°C) glass fiber filters (GF/F, 0.7 μm nominal pore size; Whatman, Maidstone, UK) and stored at -20°C. After drying the filters over night at 60°C, analysis was performed using a gas chromatograph CHNS-O elemental analyzer (Euro EA 3000, HEKAtech). Daily production rates of POC were obtained by multiplication of the respective elemental quota with corresponding specific growth rates. Chlorophyll *a* (Chl *a*) samples were filtered on GF/F filters, which were shock-frozen in liquid nitrogen and stored at -80°C. For analysis, chlorophyll was extracted in 10 mL acetone (70%) overnight at 4°C and measured fluorometrically (TD-700, Turner Designs), including an acidification step (1 M HCl) to determine phaeopigments (Knap et al. 1996). To determine biogenic silica (bSi), samples were filtered onto 0.8 μm cellulose-nitrate filters (Sartorius stedim) and stored at -20°C until measurement. Biogenic silica was determined spectrophotometrically after treatment with a molybdate solution as described in Koroleff (1983).

Statistical analysis and data fitting

All data values are given as the means of biological replicates $\pm$ SD (Tables 1, 2, 3). Statistical analysis and figure plotting were performed with the program Sigmaplot (version 12.5; Systat Software, San Jose, California, U.S.A.).

Temperature and CO_2 effects on ecophysiological parameters within each strain were analyzed applying two-way ANOVAs along with post-hoc *t*-tests using the Holm-Sidak method (both with a significance level of 0.05). Normal distribution was confirmed by a Shapiro–Wilk-test in the majority of cases. Two-way ANOVAs of those datasets with failed normality tests were run again after transformation by $ln_e()$ and passed accordingly. In order to detect gradual CO_2 responses, we additionally applied simple linear regression analyses as a function of pCO_2 to the ecophysiological responses at both temperature levels and in both strains for growth, cellular quotas and production rates. In most cases, trait values were significantly lower under a pCO_2 of 180 μatm compared to 370 μatm, while values gradually declined with further increases in pCO_2. To focus on these trends, we fitted only the data from present to future pCO_2 levels in the linear regression analysis.

Results

Species composition within community incubation experiments

Phytoplankton species composition at the start of the community incubation was diverse (> 20 species, *see* Supporting Information Table 2), representing three functional groups: diatoms, dinoflagellates, and picoeukaryotes. Over the course of the experiment, diatoms became even more dominant and represented between 87% and 98% of the final total biovolume (Table 2). Nonetheless, diversity remained high with > 15 species present in each bottle

Table 2. Percentage contribution of all diatoms and *T. hyalina* alone to the final phytoplankton assemblages of the community incubation experiment under different temperatures, pCO_2 levels as well as low (LL) and high (HL) light levels. Values are the mean and standard deviation of the three replica incubations of each treatment. The treatments which the two strains were isolated from are printed in bold.

Treatment (°C, µatm, light)			Diatoms [% biovolume]	*T. hyalina* [% biovolume]	*T. hyalina* [% cell count]
3°C	**400**	**LL**	**93 ± 3**	**36 ± 13**	**5 ± 1**
3°C	1000	LL	90 ± 13	25 ± 29	3 ± 4
3°C	400	HL	98 ± 2	49 ± 3	11 ± 2
3°C	1000	HL	98 ± 1	58 ± 15	14 ± 4
6°C	400	LL	87 ± 14	9 ± 3	1 ± 1
6°C	1000	LL	95 ± 3	10 ± 4	1 ± 1
6°C	400	HL	96 ± 3	49 ± 6	9 ± 1
6°C	**1000**	**HL**	**98 ± 1**	**52 ± 16**	**13 ± 5**

throughout the experiment. In the final assemblages, the most dominant species in terms of biovolume was *T. hyalina* (Table 2). Other important species were *Chaetoceros socialis*, *Micromonas pusilla*, *Thalassiosira concaviscula*, and *Phaeocystis pouchetii*. Despite strong differences in physicochemical conditions, however, the relative contribution of *T. hyalina* in terms of biovolume was not significantly different in the present-day (36% ± 13%) compared to the future scenario (52% ± 16%), the two treatments from which the strains were isolated. *T. hyalina* seemed to benefit from high light, particularly under higher temperatures. Under high light, i.e., the conditions closest to those of the subsequent experiments with the single strain isolates, biovolume contribution of *T. hyalina* were even more similar with 49% ± 3% under low and 52% ± 16% under high temperature and pCO_2 levels (Table 2).

Responses in single strain experiments
Growth rates

In both strains, CPL (i.e., selected under present-day conditions) and WFH (selected under future conditions), specific growth rates were very similar at 3°C (Table 3, CPL mean $\mu = 1.01 \pm 0.03$ d^{-1}, WFH: mean $\mu = 1.0 \pm 0.08$ d^{-1}) and increased significantly with temperature (Fig. 2; two-way-ANOVA, $F = 1047$; $p < 0.001$ and $F = 53$; $p < 0.001$). The temperature-dependent stimulation in growth, however, differed notably between strains with an increase of 14% in the CPL strain and 37% in the WFH strain, the latter reaching values as high as 1.44 d^{-1} (Table 3). At high temperature, the CPL strain hence grew slower and had lower biomass contents than the WFH strain. Also CO_2 treatments had significant effects on growth, yet exclusively at the temperature that the respective strain was originally isolated from: In the CPL strain only at 3°C, growth had an optimum at 370 µatm and exhibited a negative trend with further increases in pCO_2 (Fig. 2A, $r^2 = 0.45$; $p = 0.02$; $n = 9$). In the WFH strain, the opposite trend was observed, with increasing growth at higher pCO_2 at 6°C but not at 3°C (Fig. 2B, $r^2 = 0.45$; $p = 0.018$; $n = 9$). Here, growth had its optimum at

1400 µatm and was significantly higher than in all other pCO_2 treatments (two-way-ANOVA, post-hoc-test against 1000 µatm, $t = 3.2$; $p = 0.025$).

Particulate organic carbon

In the CPL strain, POC production significantly dropped on average by 48% under 6°C compared to 3°C (Fig. 2C, two-way-ANOVA, $F = 78$; $p < 0.001$). A similar effect was visible in POC quota (Table 3, two-way-ANOVA, $F = 143$; $p < 0.001$). Both traits also displayed a declining trend with increasing pCO_2 regardless of temperature (Fig. 2C; Table 3, POC quota at 3°C: $r^2 = 0.59$; $p = 0.026$; $n = 8$, POC quota at 6°C: $r^2 = 0.60$; $p = 0.015$; $n = 9$).

The WFH strain showed opposing responses compared to the CPL strain. POC production significantly increased with temperature, on average by 80% (Fig. 2D, two-way-ANOVA, $F = 424$; $p < 0.001$). Also POC quota increased significantly with temperature (Table 3, two-way-ANOVA, $F = 67$; $p < 0.001$). Although CO_2 effects were not significant, a positive trend in POC quota and production rates with increasing pCO_2 could be observed in the higher temperature treatment (Fig. 2D; Table 3). The higher POC quota in the WFH strain under future conditions could not be explained by its slightly higher cell volume compared to the CPL strain (mean POC per volume: CPL 3°C: 0.24 ± 0.02 pg POC µm^{-3}; CPL 6°C: 0.13 ± 0.02 pg POC µm^{-3}; WFH 3°C: 0.17 ± 0.001 pg POC µm^{-3}; WFH 6°C: 0.19 ± 0.01 pg POC µm^{-3}). PON quotas developed similarly to POC (data not shown), but C : N ratios were still significantly higher at 6°C than at 3°C (Table 3, two-way-ANOVA, $F = 103$; $p < 0.001$). At both temperatures, C : N ratios of the WFH strain increased slightly with rising pCO_2 (Table 3, 6°C: $r^2 = 0.40$; $p = 0.026$; $n = 12$; 3°C: $r^2 = 0.58$; $p = 0.007$; $n = 12$), again contrasting the CPL strain's response.

Chlorophyll a

In the CPL strain, cellular Chl *a* quotas were lower than in the WFH strain in all treatments. Chl *a* quota in the former were reduced by 57% under 6°C compared to 3°C (Fig. 3A, two-way-ANOVA, $F = 71$; $p < 0.001$), while increasing pCO_2 levels caused a declining trend at high temperatures

Table 3. Growth rates and cellular composition with of all cell quotas as mean and standard deviation of the respective three treatment replica of each strain.

Strain/treatment			μ [d^{-1}]	POC [pg cell^{-1}]	Chl *a* [pg cell^{-1}]	bSi [pg cell^{-1}]	C : N [mol : mol]
CPL	3°C	180	1.02 ± 0.01	263 ± 24	5.9 ± 0.7	142 ± 15	5.24 ± 0.03
		370	1.06 ± 0.04	316 ± 22	9.7 ± 0.5	212 ± 21	5.25 ± 0.05
		1000	1.0 ± 0.05	265 ± 18	8.3 ± 0.6	156 ± 16	5.19 ± 0.06
		1400	0.97 ± 0.01	261 ± 34	8.6 ± 0.9	152 ± 22	5.27 ± 0
CPL	6°C	180	1.13 ± 0.09	110 ± 22	4.1 ± 0.9	87 ± 16	4.87 ± 0.11
		370	1.17 ± 0.08	169 ± 13	6.1 ± 0.3	106 ± 8	4.98 ± 0.07
		1000	1.16 ± 0.00	154 ± 9	4.6 ± 0.7	88 ± 14	4.83 ± 0.06
		1400	1.16 ± 0.03	116 ± 18	4.4 ± 0.9	81 ± 5	5.0 ± 0.04
WFH	3°C	180	1.0 ± 0.02	320 ± 8	10.0 ± 0.3	348 ± 50	4.9 ± 0.02
		370	0.98 ± 0.01	314 ± 15	9.9 ± 0.4	418 ± 126	4.62 ± 0.4
		1000	1.03 ± 0.02	327 ± 4	10.1 ± 0.4	368 ± 41	5.09 ± 0.04
		1400	0.98 ± 0.04	323 ± 10	11.5 ± 2.3	447 ± 51	5.09 ± 0.06
WFH	6°C	180	1.36 ± 0.03	371 ± 46	9.1 ± 1.0	359 ± 101	5.19 ± 0.1
		370	1.31 ± 0.02	404 ± 11	9.7 ± 0.5	496 ± 81	5.36 ± 0.1
		1000	1.36 ± 0.04	415 ± 35	9.8 ± 0.4	440 ± 14	5.41 ± 0.11
		1400	1.44 ± 0.03	380 ± 8	9.0 ± 0.5	376 ± 15	5.43 ± 0.11

CPL: present-day-selected strain; WFH: future-selected strain.

(Fig. 3A; 6°C: $r^2 = 0.60$; $p = 0.015$; $n = 9$). Due to the concurrent decline in POC quota, however, Chl *a* : POC ratio increased significantly with temperature (Fig. 3C; two-way-ANOVA, $F = 112$; $p < 0.001$), while the CO_2 effect on Chl *a* disappeared when normalized to POC (Fig. 3C).

In the WFH strain, Chl *a* quota and even more so the Chl *a* : POC ratio decreased significantly under 6°C compared to 3°C (Fig. 3B,D; two-way-ANOVA, $F = 131$ and $F = 112$; $p < 0.001$ for both). In this strain, no significant CO_2 effects on pigment content were observed.

Biogenic silica

Strains differed strongly in biogenic silica (bSi) quota, far more than in any other measured trait. The WFH strain contained on average more than twice as much biogenic silica as the CPL strain at 3°C, and even 4 times as much at 6°C (Fig. 4A,B; Table 3). Although strains differed slightly in average size, this cannot explain the observed differences in silification. In fact, when bSi was normalized to volume or surface area (Hillebrand et al. 1999), the same patterns were observed (CPL 3°C: 0.12 ± 0.02 pg bSi μm^{-2}; 0.07 ± 0.01 pg bSi μm^{-3}, CPL 6°C: 0.07 ± 0.01 pg bSi μm^{-2}; 0.04 ± 0.005 pg bSi μm^{-3}; WFH 3°C: 0.22 ± 0.02 pg bSi μm^{-2}; 0.1 ± 0.01 pg bSi μm^{-3}; WFH 6°C: 0.21 ± 0.03 pg bSi μm^{-2}; 0.1 ± 0.01 pg bSi μm^{-3}).
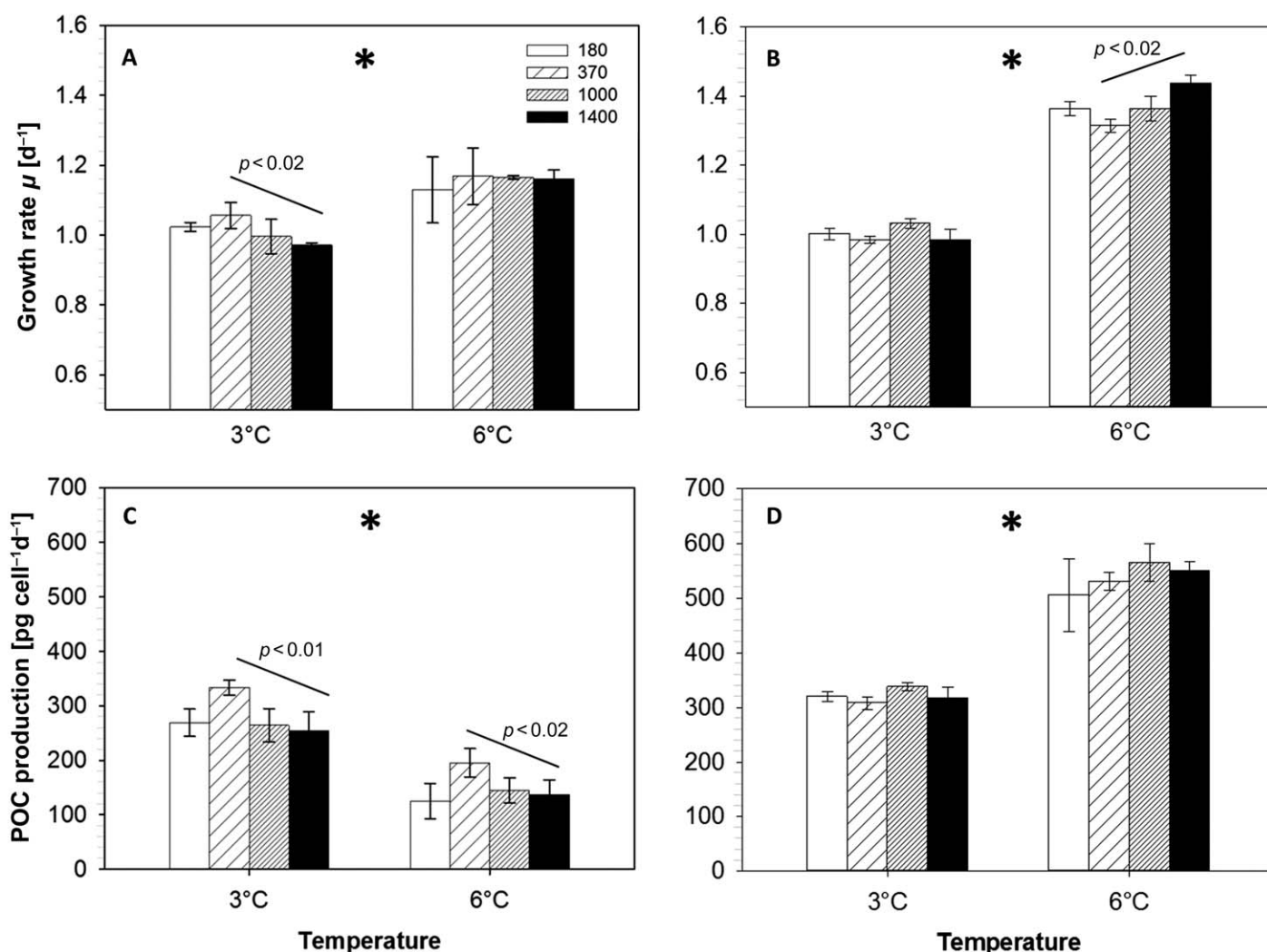
In the CPL strain, values of bSi quota were significantly lower under warmer conditions (Fig. 4A, two-way-ANOVA on quota: $F = 84$; $p < 0.001$) and decreased with increasing pCO_2 levels, similarly to POC quota (Fig. 4A,C 3°C: $r^2 = 0.69$; $p = 0.01$; $n = 8$; 6°C: $r^2 = 0.60$; $p = 0.014$; $n = 9$). The CPL strain thus revealed an optimum for bSi quota at 370 μatm pCO_2, especially at 3°C.

In the WFH strain, silica quota did not differ significantly between temperatures (Fig. 4B). Under warm conditions, bSi quota showed a decreasing trend with rising pCO_2 (Table 3, bSi quota: $r^2 = 0.59$; $p = 0.015$; $n = 9$), while such a response was not observed at 3°C. Also in the ratio of bSi : POC, a significant difference between temperature treatments was observed: less silica was measured per carbon unit at 6° compared to 3°C (Fig. 4D; two-way-ANOVA, $F = 124$; $p < 0.001$). Along with bSi quota, bSi : POC also declined under increasing pCO_2 levels (Fig. 4B,D; $r^2 = 0.51$; $p = 0.03$; $n = 9$).

Discussion

Stability of community structure under contrasting environmental conditions

Studies of phytoplankton responses to climate change are often motivated by the question how shifts in distribution of species and functional groups will impact the higher trophic levels as well as biogeochemical cycles. Also in the Arctic, field studies suggest major shifts in phytoplankton assemblages to occur as a consequence of ocean change (e.g., Li et al. 2009; Hegseth and Tverberg 2013). In contrast, we did not observe significant changes in the final composition of our community experiment in response to ocean warming, acidification and higher irradiance (Table 2). This is especially surprising since experimental approaches very similar to ours have yielded strong species shifts in the Southern Ocean (e.g., Tortell et al. 2008; Feng et al. 2010; Hoppe et al. 2013). Diatoms typically dominate in such experiments under nutrient-replete conditions in high-latitude oceans (Hoppe et al. 2017). At the end of incubation (10–30 d), however, these studies always showed a clear dominance of few species.

Fig. 2. Growth rate constants (**A**, **B**) and POC production (**C**, **D**) of the CPL strain (**A**, **C**) and the WFH strain (**B**, **D**). CO_2 treatments (180 μatm, 370 μatm, 1000 μatm, 1400 μatm) are depicted as increasingly shaded bars. Significant differences between the average of temperature treatments are denoted as * (two-way-ANOVA, level of significance $\alpha = 0.05$). Significant trends between 370 μatm and 1400 μatm are marked as lines with respective *p*-value).
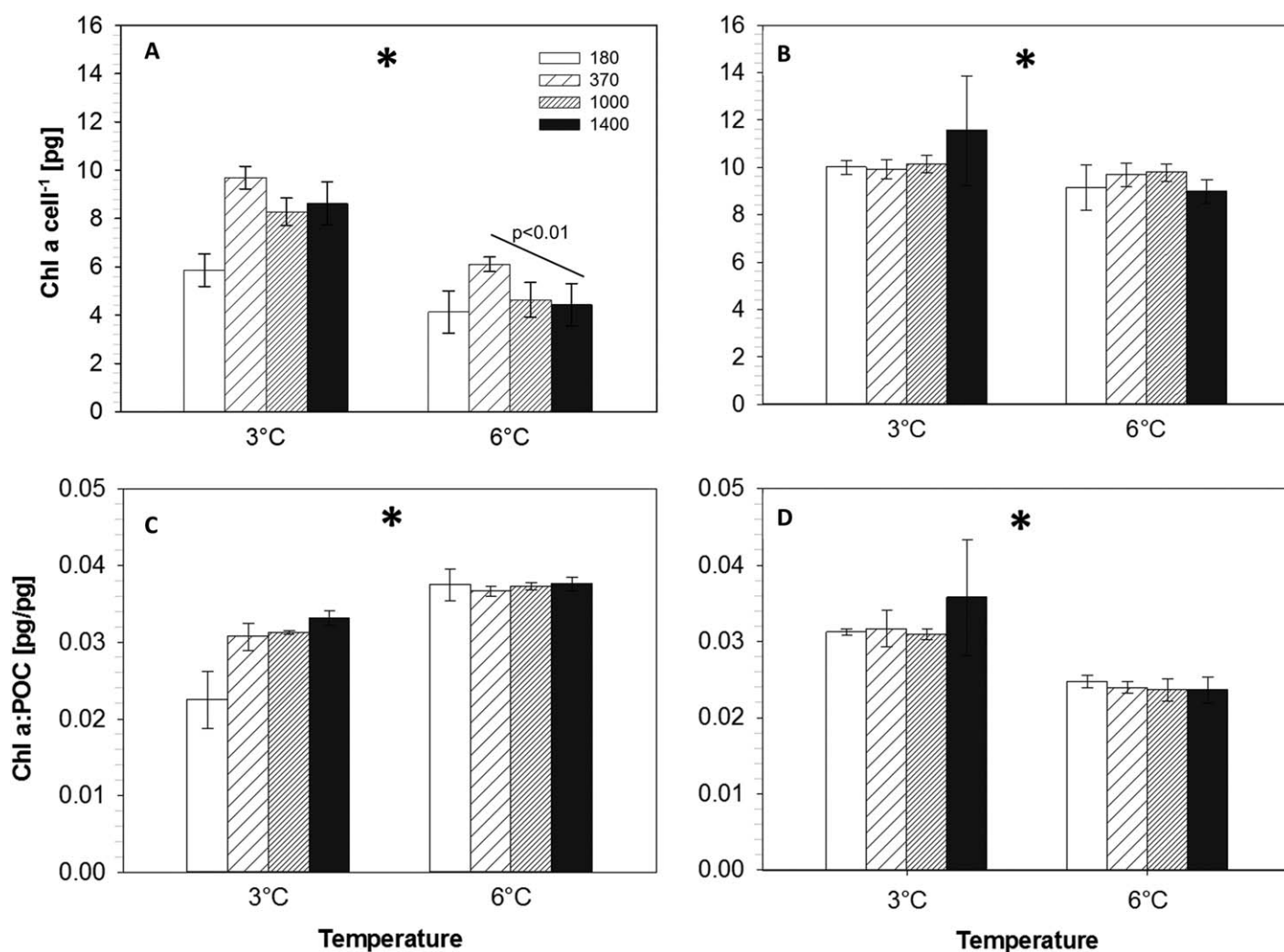
In the current community incubation, a higher level of diversity was retained throughout the experiment, with the most dominant species (*T. hyalina*, *C. socialis*, and *Micromonas pouchetii*) together accounting for only 57–88% of the total cell count and 25–70% of the total biovolume (data not shown). Furthermore, the most important species, *T. hyalina*, did not show significant differences in its dominance even in the most extreme treatments, i.e., the present-day and the future scenario. Thus, there seem to be processes at work that helped stabilizing the community composition and diversity despite strong changes in environmental conditions (Connell and Ghedini 2015). We hypothesized that these processes could include adjustments on the population level. The concurrent strain isolation and subsequent experiments were conducted to test whether intraspecific differences in physiological plasticity could be high enough to favor sorting between strains of *T. hyalina* over species shifts.

Fast growth and high temperature optima for a polar species

It is well understood that temperature responses usually follow an optimum curve (e.g., Kingsolver 2009). Even though we tested only two temperature scenarios here, our results imply that optimum temperatures for growth of both *T. hyalina* strains must be found at or even above 6°C (Fig. 2A,B). Additional incubations with the WFH strain at 8°C have indeed shown that growth rates increased even further (data not shown). In view of the spring temperatures prevailing in the Kongsfjord, ranging from −1°C to 4°C (April–June; Hegseth, in press), *T. hyalina* seem to dwell at the lower end of a surprisingly wide temperature tolerance range.

Higher performance under temperatures exceeding those typical for their environment has been reported in Southern Ocean and Arctic diatoms (Reay et al. 1999; Pančić et al. 2015; Schlie and Karsten 2016), illustrating that a direct

Fig. 3. Chl *a* quota (**A**, **B**) and Chl *a* : POC ratio (**C**, **D**) of the CPL strain (**A**, **C**) and the WFH strain (**B**, **D**). CO_2 treatments (180 μatm, 370 μatm, 1000 μatm, 1400 μatm) are depicted as increasingly shaded bars. Significant differences between the average of temperature treatments are denoted as * (two-way-ANOVA, level of significance $\alpha = 0.05$). Significant trends between 370 μatm and 1400 μatm are marked as lines with respective *p*-value.
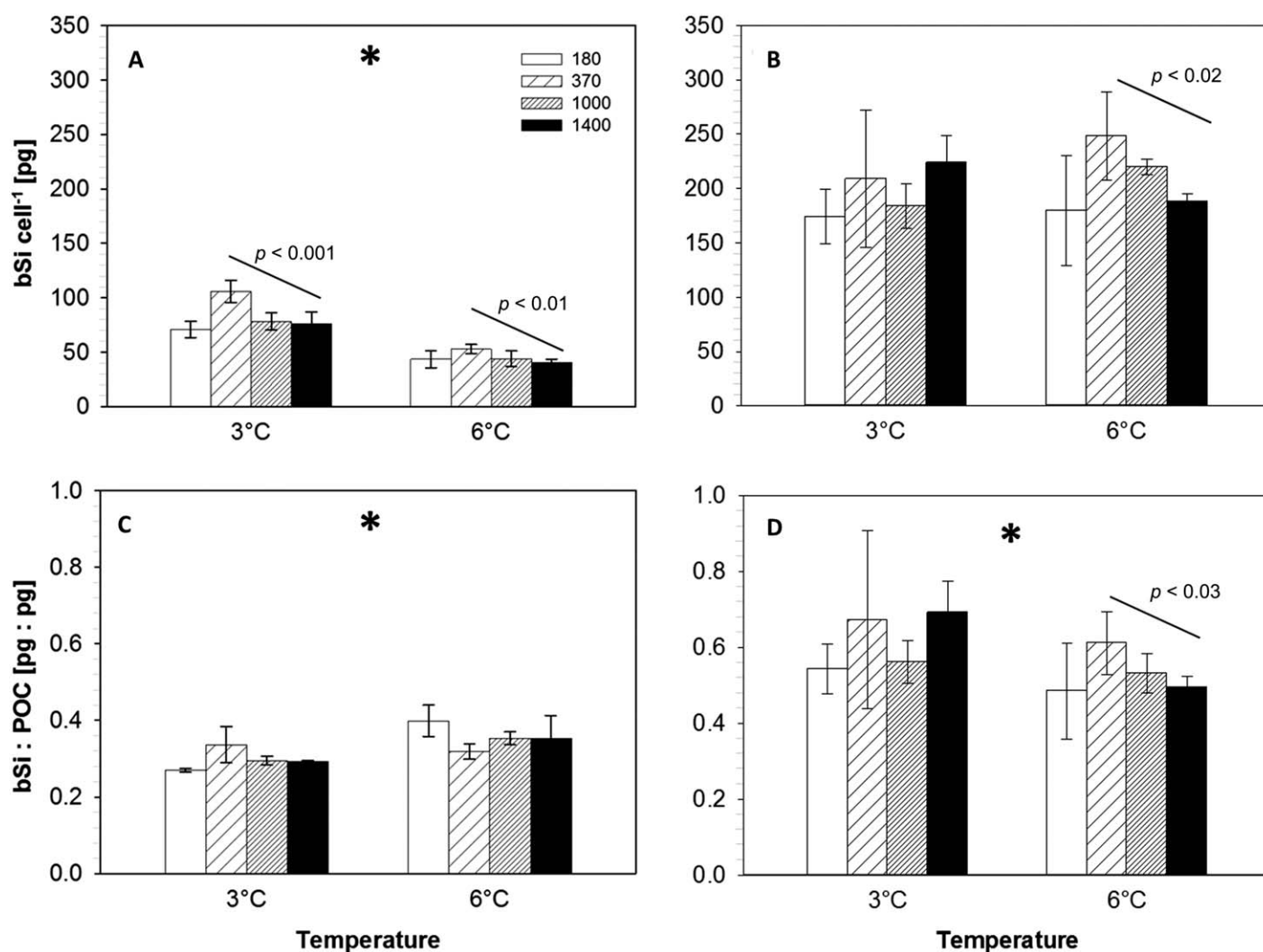
correlation of a species' geographical location and its optimal growth conditions is not always applicable (Boyd 2013). Especially in extreme environments like polar oceans, the habitat of an organism is not necessarily defined by their optimal temperature range but may be merely their realized niche in context of other biotic factors (like competitors and predators; cf. Litchman et al. 2012).

Based on an eco-evolutionary model, Thomas et al. (2012) concluded that polar phytoplankton may indeed be less vulnerable to global warming compared to species from warmer regions. The specific growth rates observed in this study (mean $\mu = 1.0$–1.36 d^{-1}) are among the highest ever reported in polar diatoms (cf. Montagnes and Franklin 2001; Pančić et al. 2015; Schlie and Karsten 2016) and are even comparable to those of temperate species (Sarthou et al. 2005; Thomas et al. 2012). In some cases (i.e., 6°C treatments in the WFH strain), they even exceed the typical temperature vs.

growth relationships of phytoplankton (cf. Eppley 1972; Bissinger et al. 2008), and thus challenge the very limits of theoretical physiological feasibility (Flynn and Raven 2016). Importantly, we also show that this is not true to the same extent for every individual of a population.

Strain-specific responses to warming and ocean acidification

Provided that an organism is living below its optimum temperature today, which is apparently the case for the here investigated strains of *T. hyalina*, all cellular process rates should be stimulated by moderate warming because of faster enzyme kinetics (Q10-law). Growth clearly increased under higher temperature in both strains, even though to a notably larger degree in the strain isolated from future conditions (i.e., WFH; Fig. 2A,B). POC production under elevated temperature, on the other hand, developed in opposite directions in

Fig. 4. bSi quota (**A**, **B**) and bSi : POC ratio (**C**, **D**) of the CPL strain (**A**, **C**) and the WFH strain (**B**, **D**). CO_2 treatments (180 μatm, 370 μatm, 1000 μatm, 1400 μatm) are depicted as increasingly shaded bars. Significant differences between the average of temperature treatments are denoted as * (two-way-ANOVA, level of significance $\alpha = 0.05$). Significant trends between 370 μatm and 1400 μatm are marked as lines with respective *p*-value.

the two strains: While the strain isolated from present-day conditions (i.e., CPL) reduced its POC production as well as quota by more than 50%, the WFH strain appeared to benefit greatly in terms of carbon production (67%) and quota (22%) under the same conditions (Fig. 2C,D; Table 3). Hence, the CPL strain was apparently not able to balance cell division and carbon fixation under elevated temperature, while the WFH strain managed to increase both processes.

The Chl *a* : POC ratios also changed in opposite directions in the two strains, being higher in the CPL strain and lower in the WFH strain under elevated temperature. Changes in this ratio have been interpreted as an indicator of photosynthetic efficiency (Rokitta and Rost 2012), since it demonstrates how much chlorophyll is needed for the fixation or storage of a carbon unit. According to these considerations, the efficiency of energy conversion into biomass

decreased with temperature in the CPL strain, while it increased in the WFH strain (Fig. 3C,D), corroborating that the latter benefits more than the first from warming.

CO_2 effects were more subtle than those of warming, which is not surprising given that relatively high tolerance toward variable pH has previously been reported in Arctic diatoms (Pančić et al. 2015). The ability to withstand changes in the surrounding pH is to be expected in these organisms, since coastal Arctic waters can display fairly large seasonal pH fluctuations (Thoisen et al. 2015). Nevertheless, having resolved a wide array of pH-treatments ($\sim$ 7.5–8.3), the observed effects have important implications concerning the individual optima of the two strains. In growth and most other measured traits, high pCO$_2$ had a negative effect on the CPL strain but slightly positive or no impacts on the WFH strain. This suggests firstly that *T. hyalina*'s tolerance

range for pCO_2 is wide, but also that optima differ intra-specifically, lying close to today's values in case of the CPL strain and even above those for the WFH strain: While growth rates of the WFH strain were stimulated by high pCO_2 treatments (Fig. 2B), cell quota of POC and Chl *a* were not significantly affected (Figs. 2D, 3B; Table 3). In the CPL strain, on the other hand, the latter parameters all decreased significantly at elevated pCO_2 (Figs. 2C, 3A; Table 3). This may hint toward a negative effect of both elevated tempera-ture and pCO_2 on biomass buildup of the CPL strain. Yet, due to the plasticity in its quota, it was still able to slightly increase its growth rate. In other words, physiological reorga-nization in this strain may have been necessary in order to meet the challenge of maintaining high growth under sub-optimal circumstances.

Next to the responses to warming and pCO_2 alone, signif-icant interactive effects were also evident. In case of specific growth rates, optimal CO_2-windows differed not only between strains but were also modulated by temperature: Growing under warmer conditions, both strains appeared to cope better with or even profit from elevated pCO_2 (Fig. 2A,B), causing the optimum range to widen and to move to higher pCO_2 levels. Such an upward shift in the CO_2 opti-mum at higher temperatures has also been described for coc-colithophores (Sett et al. 2014). Hence, a higher ability to cope with OA under modest warming may be a general response pattern of phytoplankton. Furthermore, these results demonstrate that it is indispensable to consider inter-active effects of multiple stressors on an organism in order to judge their capabilities (e.g., Rost et al. 2008). Even within this experiment, for example, CO_2 responses of growth rates would seem contradictive unless taking interactions with temperature and the possibility of shifted reaction norms into account.

The higher growth rates induced in both investigated strains under future conditions may, however, come with potential tradeoffs. Under current Svalbard spring condi-tions, growth rates of both strains were very similar, which can explain why both phenotypes coexist today. At the same time, both strains were seemingly capable of coping with conditions exceeding scenarios predicted for the next 100 yr. However, they may not be equally competitive under those conditions. The CPL strain was unable to increase its growth as much as the WFH strain and maintained it only at the expense of lowered biomass build-up. Such lower carbon storage, as observed under future conditions, could translate to a lower resilience against longer phases of sub-optimal conditions (e.g., light limitation) or the formation of resting spores with smaller energy reserves and thus lower hatching success. The WFH strain, on the other hand, increased both, growth and carbon quota simultaneously.

According to our data, the CPL strain revealed an opti-mum of all parameters under a present-day setting, while the WFH strain was found to have its optima at higher temperatures and pCO_2 levels. Therefore, the CPL strain would likely be outcompeted in such a scenario, not only because of its relatively lower growth rate but also because of its overall physiological performance. This considered, abso-lute growth rate in isolation should be interpreted only with some caution as a direct indicator of ecological competitive-ness (cf. Schaum and Collins 2014). Nonetheless, it is still the best fitness-determining parameter at hand (Collins et al. 2013).

Intraspecific diversity as the basis for rapid evolution

The differences between the strains illustrate that even when interactive effects and optimum curves are taken into account, the prediction of responses to environmental change must consider another factor: the standing stock of individual strains with diverse optimum curves. Considering the treatments of the community experiments, which the strains had been isolated from, the observed reaction norms match the respective former selection environment remark-ably well. This is particularly astonishing because both cell lineages originate from a single water sample, i.e., the same pre-spring-bloom community. It shows that within a single species or even population, individuals can differ greatly in their reaction norms and respective optima, which is in agreement with the old paradigm of Baas-Becking (1934) that "everything is everywhere but environment selects." Consequently, the true range of plasticity within a popula-tion needs to be assumed much larger than a single strain may indicate. Given the existence of many locally distinct populations, the plasticity of a whole species or functional group must be even greater. Already on a local level, several interconnected populations can contribute to the diversity pool of one assemblage (Chen and Rynearson 2016). This may also be the case in our study site, the Kongsfjord, which is being influenced by both Arctic and Atlantic water masses potentially carrying different populations into the fjord (Hegseth and Tverberg 2013). Irrespective of the population structure at our study site, knowledge on intraspecific diver-sity is mandatory when upscaling results from the laboratory.

Even though we cannot be certain that our two strains actually represent the dominant phenotypes in their respec-tive isolation environments, the observed growth rates and the associated stochastic probabilities render it likely that our experimental design may indeed have selected for indi-viduals with very different response optima. Having tested only two individuals in detail, our study is certainly no reli-able representation of the existing diversity, but it can serve as a documentation of the minimum variability that can be present in the population. The observed difference in growth rate between the two strains under future conditions was 0.2 d^{-1} and thus sufficiently different to have caused substantial deviations in cell densities between the two strains at the end of our incubations. If this selection of differing strains

within our experimental population actually did happen, it may reveal a mechanism for adaptation on the more cryptic intraspecific level. The wider implications of such small-scale considerations have recently been explored in a game-theoretic model by Menden-Deuer and Rowlett (2014). Given our incubation times of only 10–13 d, this mechanism may operate on extremely short timescales. The lack of significant species shifts within our community incubation experiment despite severe alterations in environmental conditions (Table 1) could in fact be explained by this surprisingly high intraspecific plasticity and sorting of strains with the respective optima. Our results therefore indicate that present-day populations of *T. hyalina* already have the potential to adapt efficiently to future conditions, provided the standing diversity is sufficiently large (Collins et al. 2013). Although species shifts within the community could thus be evaded up to a certain degree of environmental change, alterations of the average population characteristics would still be a likely consequence.

Biogeochemical implications

While we do expect intraspecific diversity to remain high under future conditions, successful individuals are still more likely to have trait characteristics resembling those of our WFH strain. Thus, in a bravely up-scaled scenario, our data suggest that *T. hyalina* populations would grow faster (Fig. 2B), become more efficient in photosynthesis (Chl a : POC ratio; Fig. 3D) and have higher carbon storage (POC quota; Table 3). On the ecosystem level, such changes could translate to higher overall primary and oxygen production. Faster growth rates may also speed up bloom dynamics, which can give the population a head-start to subsequent grazer population (Assmy and Smetacek 2009), thus changing modes and dynamics of carbon recycling and export to depth.

Increased sinking rates could also be anticipated because of the ballasting effect of the fourfold higher silica content of the WFH strain compared to the CPL strain (Fig. 4A,B). In addition, POC density itself was higher in the WFH strain under future conditions (*see* "Results" section). These two effects could induce a more efficient carbon export production, thus increasing *T. hyalina*'s contribution to the biological carbon pump. The impressively large difference in silification of the two strains may also have an impact on their vulnerability to grazing (Hamm and Smetacek 2007). This being said, biogenic silica was the only parameter showing a decreasing trend under high CO_2 conditions in both strains (except for 3°C in WFH, Fig. 4B). This could indicate that diatom bSi quota may generally tend to decrease under future CO_2 conditions, a trend which has been observed before (Milligan et al. 2004; Hervé et al. 2012; Hoppe et al. 2015). Further elucidation of the underlying physiological mechanisms and associated tradeoffs of such responses may eventually allow identifying those strain properties acting as a driving force for population dynamics.

The few hard data available for parametrization of ecological and earth system models usually originates from single-strain lab experiments. At the same time, such models often treat phytoplankton merely on the level of bulk properties of a few functional groups (Follows and Dutkiewicz 2011). More specialized models trying to integrate intraspecific diversity into the forecasting of species shifts face a vast lack of empirical data and conceptual understanding (Valladares et al. 2014). Physiological reaction norms that take the true spread of traits within a species into account are therefore increasingly called for (e.g., Hattich et al. 2017). Ultimately, study designs like the one presented here (*see* Fig. 1) could therefore help to establish more realistic reaction norms of phytoplankton groups and to develop more advanced model parametrization for understanding current and future ecosystem dynamics.

Conclusions

The novelty of our study design is the combination of a phytoplankton community-based experiment followed by monoculture-based laboratory experiments with individuals originating from these specific selection environments. The work with single strains is indispensable when investigating phenotypic plasticity and can also provide mechanistic understanding of the underlying physiology. Our methodological framework, however, holds the potential not to randomly pick strains from the population, but to "pre-select" them based on those traits that are beneficial under specific environmental scenarios. This approach may prove useful for specific investigations on the far ends of a community's tolerance range. While we cannot claim to actually capture the full range of plasticity within the *T. hyalina* population, our study shows an impressive intraspecific spread of trait optima that depicts at least the minimum range that must be present within a single water sample.

References

AMAP. 2013. Assessment 2013: Arctic Ocean acidification. Arctic Monitoring and Assessment Programme (AMAP), p. viii + 99 pp.

Assmy, P., and V. Smetacek. 2009. Algal blooms, p. 27–41. *In* M. Schaechter [ed.], Encyclopedia of microbiology. Elsevier.

Baas-Becking, L. G. M. 1934. Geobiologie; of inleiding tot de milieukunde. WP Van Stockum & Zoon NV.

Beszczynska-Möller, A., U. Schauer, E. Fahrbach, and E. Hansen. 2013. Variability of the Atlantic water properties and oceanic fluxes in the entrance to the Arctic Ocean - causes and consequences, p. 12962. EGU General Assembly Conference Abstracts.

Bissinger, J. E., D. J. Montagnes, J. Sharples, and D. Atkinson. 2008. Predicting marine phytoplankton maximum growth rates from temperature: Improving on the

Eppley curve using quantile regression. Limnol. Oceanogr. **53**: 487. doi:10.4319/lo.2008.53.2.0487

Boyd, P. W. 2013. Framing biological responses to a changing ocean. Nat. Clim. Chang. **3**: 530–533. doi:10.1038/nclimate1881

Brand, L. E. 1989. Review of genetic variation in marine phytoplankton species and the ecological implications. Biol. Oceanogr. **6**: 397–409.

Brewer, P. G., A. L. Bradshaw, and R. T. Williams. 1986. Measurement of total carbon dioxide and alkalinity in the North Atlantic ocean in 1981, p. 358–381. *In* J. R. Trabalka, and D. E. Reichle [eds.], The Changing Carbon Cycle – A Global Analysis Springer Verlag.

Casteleyn, G., K. M. Evans, T. Backeljau, S. D'hondt, V. A. Chepurnov, K. Sabbe, and W. Vyverman. 2009. Lack of population genetic structuring in the marine planktonic diatom *Pseudo-nitzschia pungens* (Bacillariophyceae) in a heterogeneous area in the Southern Bight of the North Sea. Mar. Biol. **156**: 1149–1158. doi:10.1007/s00227-009-1157-6

Chen, G., and T. A. Rynearson. 2016. Genetically distinct populations of a diatom co-exist during the North Atlantic spring bloom. Limnol. Oceanogr. **61**: 2165–2179. doi:10.1002/lno.10361

Coello-Camba, A., S. Agustí, J. Holding, J. M. Arrieta, and C. M. Duarte. 2014. Interactive effect of temperature and CO_2 increase in Arctic phytoplankton. Front. Mar. Sci. **1**: 49. doi:10.3389/fmars.2014.00049

Collins, S., B. Rost, and T. A. Rynearson. 2013. Evolutionary potential of marine phytoplankton under ocean acidification. Evol. Appl. **7**: 140–155. doi:10.1111/eva.12120

Connell, S. D., and G. Ghedini. 2015. Resisting regime-shifts: The stabilising effect of compensatory processes. Trends Ecol. Evol. **30**: 513–515. doi:10.1016/j.tree.2015.06.014

Cullather, R. I., Y. K. Lim, L. N. Boisvert, L. Brucker, J. N. Lee, and S. M. Nowicki. 2016. Analysis of the warmest Arctic winter, 2015–2016. Geophys. Res. Lett. **43**: 10808–10816. doi:10.1002/2016GL071228

Dickson, A. G., and F. J. Millero. 1987. A comparison of the equilibrium constants for the dissociation of carbonic acid in seawater media. Deep-Sea Research **34**: 1733–1743. doi:10.1016/0198-0149(87)90021-5

Eppley, R. W. 1972. Temperature and phytoplankton growth in the sea. Fish. Bull. **70**: 1063–1085.

Evans, K. M., S. F. Kühn, and P. K. Hayes. 2005. High levels of genetic diversity and low levels of genetic differentiation in North Sea *Pseudo-Nitzschia pugens* (Bacillariophyceae) populations. J. Phycol. **41**: 506–514. doi:10.1111/j.1529-8817.2005.00084.x

Feng, Y., and others. 2010. Interactive effects of iron, irradiance and CO_2 on Ross Sea phytoplankton. Deep-Sea Res. Part I Oceanogr. Res. Pap. **57**: 368–383. doi:10.1016/j.dsr.2009.10.013

Field, C. B., M. J. Behrenfeld, J. T. Randerson, and P. Falkowski. 1998. Primary production of the biosphere: Integrating terrestrial and oceanic components. Science **281**: 237–240. doi:10.1126/science.281.5374.237

Flynn, K. J., and J. A. Raven. 2016. What is the limit for photoautotrophic plankton growth rates? J. Plankton Res. **39**: 13–22. doi:10.1038/Nclimate2768

Follows, M. J., and S. Dutkiewicz. 2011. Modeling diverse communities of marine microbes. Annu. Rev. Mar. Sci. **3**: 427–451. doi:10.1146/annurev-marine-120709-142848

Gao, K., E. W. Helbling, D.-P. Häder, and D. A. Hutchins. 2012. Responses of marine primary producers to interactions between ocean acidification, solar radiation, and warming. Mar. Ecol. Prog. Ser. **470**: 167–189. doi:10.3354/meps10043

Gao, K., and D. A. Campbell. 2014. Photophysiological responses of marine diatoms to elevated CO_2 and decreased pH: A review. Funct. Plant Biol. **41**: 449. doi:10.1071/FP13247

Guillard, R. R. L., and J. H. Ryther. 1962. Studies of marine planktonic diatoms. I. *Cyclothella nana* Hustedt and *Detonula confervacea* Cleve. Can. J. Microbiol. **8**: 229–239. doi:10.1139/m62-029

Häder, D.-P., and K. Gao. 2015. Interactions of anthropogenic stress factors on marine phytoplankton. Front. Environ. Sci. **3**: 1–14. doi:10.3389/fenvs.2015.00014

Hamm, C., and V. Smetacek. 2007. Armor: Why, when, and how, p. 311–332. *In* P. Falkowski and A. Knoll [eds.], Evolution of primary producers in the sea. Academic Press.

Hare, C. E., K. Leblanc, G. R. DiTullio, R. M. Kudela, Y. Zhang, P. A. Lee, S. Riseman, and D. A. Hutchins. 2007. Consequences of increased temperature and CO_2 for phytoplankton community structure in the Bering Sea. Mar. Ecol. Prog. Ser. **352**: 9–16. doi:10.3354/meps07182

Härnström, K., M. Ellegaard, T. J. Andersen, and A. Godhe. 2011. Hundred years of genetic structure in a sediment revived diatom population. Proc. Natl. Acad. Sci. USA **108**: 4252–4257. doi:10.1073/pnas.1013528108

Hasle, G. R., and E. E. Syvertsen. 1997. Chapter 2 - Marine diatoms, p. 5–385. *In* C. R. Tomas [ed.], Identifying marine phytoplankton. Academic Press.

Hattich, G. S., L. Listmann, J. Raab, D. Ozod-Seradj, T. B. Reusch, and B. Matthiessen. 2017. Inter-and intraspecific phenotypic plasticity of three phytoplankton species in response to ocean acidification. Biol. Lett. **13**: 20160774. doi:10.1098/rsbl.2016.0774

Hegseth, E. N., and others. In press. Phytoplankton seasonal dynamics in Kongsfjorden, Svalbard and the adjacent shelf. *In* H. Hop, and C. Wiencke [eds.], The Ecosystem of Kongsfjorden, Svalbard. Advances in Polar Ecology 2. Springer Verlag.

Hegseth, E. N., and V. Tverberg. 2013. Effect of Atlantic water inflow on timing of the phytoplankton spring bloom in a high Arctic fjord (Kongsfjorden, Svalbard). J. Mar. Syst. **113–114**: 94–105. doi:10.1016/j.jmarsys.2013.01.003

Hervé, V., J. Derr, S. Douady, M. Quinet, L. Moisan, and P. J. Lopez. 2012. Multiparametric analyses reveal the pH-dependence of silicon biomineralization in diatoms. PloS one **7**: e46722. doi:10.1371/journal.pone.0046722

Hillebrand, H., C.-D. Dürselen, D. Kirschtel, U. Pollingher, and T. Zohary. 1999. Biovolume calculation for pelagic and bethic microalgae. J. Phycol. **35**: 403–424. doi: 10.1046/j.1529-8817.1999.3520403.x

Holding, J. M., and others. 2015. Temperature dependence of CO_2-enhanced primary production in the European Arctic Ocean. Nat. Clim. Chang. **5**: 1079–1082. doi:10.1038/nclimate2768

Hoppe, C. J. M., G. Langer, S. D. Rokitta, D. A. Wolf-Gladrow, and B. Rost. 2012. Implications of observed inconsistencies in carbonate chemistry measurements for ocean acidification studies. Biogeosciences **9**: 2401–2405. doi:10.5194/bg-9-2401-2012

Hoppe, C. J., C. S. Hassler, C. D. Payne, P. D. Tortell, B. Rost, and S. Trimborn. 2013. Iron limitation modulates ocean acidification effects on Southern Ocean phytoplankton communities. PloS One **8**: e79890. doi:10.1371/journal.pone.0079890

Hoppe, C. J. M., L. M. Holtz, S. Trimborn, and B. Rost. 2015. Ocean acidification decreases the light-use efficiency in an Antarctic diatom under dynamic but not constant light. New Phytologist **207**: 159–171. doi:10.1111/nph.13334

Hoppe C. J., N. Schuback, D. M. Semeniuk, M. Maldonado, and B. Rost. 2017. Functional redundancy mediates phytoplankton resilience to ocean acidification and increased irradiances. Frontiers in Marine Science **4**: 229. doi: 10.3389/fmars.2017.00229

IPCC. 2013. Climate Change 2013: The Physical Science Basis. *In* T. F. Stocker and others [eds.], Contribution of Working Group I to the Fifth Assessment Report of the Intergovernmental Panel on Climate Change, p. 1535. Cambridge Univ. Press.

Kingsolver, J. G. 2009. The well temperatured biologist (American Society of Naturalists Presidential Address). Am. Nat. **174**: 755–768. doi:10.1086/648310

Knap, A., A. Michaels, A. Close, H. Ducklow, and A. E. Dickson. 1996. Protocols for the Joint Global Ocean Flux Study (JGOFS) Core Measurements, p. 170. JGOFS Report Nr. 19. UNESCO.

Koroleff, F. 1983. Determination of silicon, p. 174–183. *In* M. E. K. Grasshoff, and K. Kremling [eds.], Methods of Seawater Analysis. Verlag Chemie.

Kranz, S. A., M. Eichner, and B. Rost. 2011. Interactions between CCM and N_2 fixation in *Trichodesmium*. Photosynth. Res. **109**: 73–84. doi:10.1007/s11120-010-9611-3

Kremp, A., A. Godhe, J. Egardt, S. Dupont, S. Suikkanen, S. Casabianca, and A. Penna. 2012. Intraspecific variability in the response of bloom-forming marine microalgae to changed climate conditions. Ecol. Evol. **2**: 1195–1207. doi:10.1002/ece3.245

Lakeman, M. B., P. von Dassow, and R. A. Cattolico. 2009. The strain concept in phytoplankton ecology. Harmful Algae **8**: 746–758. doi:10.1016/j.hal.2008.11.011

Langer, G., G. Nehrke, I. Probert, J. Ly, and P. Ziveri. 2009. Strain-specific responses of *Emiliania huxleyi* to changing

seawater carbonate chemistry. Biogeosciences **6**: 2637–2646. doi:10.5194/bg-6-2637-2009

Li, W. K. W., F. A. McLaughlin, C. Lovejoy, and E. C. Carmack. 2009. Smallest algae thrive as the arctic ocean freshens. Science **326**: 539. doi:10.1126/science.1179798

Litchman, E., K. F. Edwards, C. A. Klausmeier, and M. K. Thomas. 2012. Phytoplankton niches, traits and eco-evolutionary responses to global environmental change. Mar. Ecol. Prog. Ser. **470**: 235–248. doi:10.3354/meps09912

Mehrbach, C., C. H. Culberson, J. E. Hawley, and R. M. Pytkowicz. 1973. Measurement of the apparent dissociation constants of carbonic acid in seawater at atmospheric pressure. Limnol. Oceanogr. **18**: 897–907.

Menden-Deuer, S., and J. Rowlett. 2014. Many ways to stay in the game: Individual variability maintains high biodiversity in planktonic microorganisms. J. R. Soc. Interface **11**: 20140031. doi:10.1098/rsif.2014.0031

Menden-Deuer, S., and T. Kiørboe. 2016. Small bugs with a big impact: Linking plankton ecology with ecosystem processes. J. Plankton Res. **38**: 1036–1043. doi:10.1093/plankt/fbw049

Milligan, A. J., D. E. Varela, M. A. Brzezinski, and F. M. M. Morel. 2004. Dynamics of silicon metabolism and silicon isotopic discrimination in a marine diatom as a function of pCO_2. Limnol. Oceanogr. **49**: 322–329. doi:10.4319/lo.2004.49.2.0322

Montagnes, D. J., and M. Franklin. 2001. Effect of temperature on diatom volume, growth rate, and carbon and nitrogen content: Reconsidering some paradigms. Limnol. Oceanogr. **46**: 2008–2018. doi:10.4319/lo.2001.46.8.2008

Nöthig, E.-M., and others. 2015. Summertime plankton ecology in Fram Strait - a compilation of long- and short-term observations. Polar Res. **34**: 23349. doi:10.3402/polar.v34.23349

Pančić, M., P. J. Hansen, A. Tammilehto, and N. Lundholm. 2015. Resilience to temperature and pH changes in a future climate change scenario in six strains of the polar diatom *Fragilariopsis cylindrus*. Biogeosci. Discuss. **12**: 4627–4654. doi:10.5194/bgd-12-4627-2015

Pierrot, D. E., E. Lewis, and D. W. R. Wallace. 2006. MS Exel program developed for CO_2 system calculations. *In* O. R. N. L. ORNL/CDIAC-105a Carbon Dioxide Information Analysis Centre [ed.].

Poulin, M., N. Daugbjerg, R. Gradinger, L. Ilyash, T. Ratkova, and C. von Quillfeldt. 2011. The pan-Arctic biodiversity of marine pelagic and sea-ice unicellular eukaryotes: A first-attempt assessment. Mar. Biodivers. **41**: 13–28. doi:10.1007/s12526-010-0058-8

Reay, D. S., D. B. Nedwell, J. Priddle, and J. C. Ellis-Evans. 1999. Temperature dependence of inorganic nitrogen uptake: Reduced affinity for nitrate at suboptimal temperatures in both algae and bacteria. Appl. Environ. Microbiol. **65**: 2577–2584.

Rokitta, S. D., and B. Rost. 2012. Effects of CO_2 and their modulation by light in the life-cycle stages of the

coccolithophore *Emiliania huxleyi*. Limnol. Oceanogr. **57**: 607–618. doi:10.4319/lo.2012.57.2.0607

Rost, B., I. Zondervan, and D. Wolf-Gladrow. 2008. Sensitivity of phytoplankton to future changes in ocean carbonate chemistry: Current knowledge, contradictions and research directions. Mar. Ecol. Prog. Ser. **373**: 227–237. doi:10.3354/meps07776

Rynearson, T. A., and E. Armbrust. 2000. DNA fingerprinting reveals extensive genetic diversity in a field population of the centric diatom *Ditylum brightwellii*. Limnol. Oceanogr. **45**: 1329–1340. doi:10.4319/lo.2000.45.6.1329

Rynearson, T. A., and S. Menden-Deuer. 2016. Drivers that structure biodiversity in the plankton, p. 13–24. *In* P. M. Glibert, and T. M. Kana [eds.], Aquatic microbial ecology and biogeochemistry: A dual perspective. Springer.

Sarthou, G., K. R. Timmermans, S. Blain, and P. Tréguer. 2005. Growth physiology and fate of diatoms in the ocean: A review. J. Sea Res. **53**: 25–42. doi:10.1016/j.seares.2004.01.007

Schaum, C. E., and S. Collins. 2014. Plasticity predicts evolution in a marine alga. Proc. R. Soc. Lond. B Biol. Sci. **281**: 20141486. doi:10.1098/rspb.2014.1486

Schaum, E., B. Rost, A. J. Millar, and S. Collins. 2012. Variation in plastic responses of a globally distributed picoplankton species to ocean acidification. Nat. Clim. Chang. **3**: 298–302. doi:10.1038/nclimate1774

Schlie, C., and U. Karsten. 2016. Microphytobenthic diatoms isolated from sediments of the Adventfjorden (Svalbard): Growth as function of temperature. Polar Biol. **40**: 1043–1051. doi:10.1007/s00300-016-2030-y

Schulz, K. G., and others. 2013. Temporal biomass dynamics of an Arctic plankton bloom in response to increasing levels of atmospheric carbon dioxide. Biogeosciences (BG) **10**: 161–180. doi:10.5194/bg-10-161-2013

Sett, S., L. T. Bach, K. G. Schulz, S. Koch-Klavsen, M. Lebrato, and U. Riebesell. 2014. Temperature modulates coccolithophorid sensitivity of growth, photosynthesis and calcification to increasing seawater CO_2. PloS One **9**: e88308. doi:10.1371/journal.pone.0088308

Sildever, S., J. Sefbom, I. Lips, and A. Godhe. 2016. Competitive advantage and higher fitness in native populations of genetically structured planktonic diatoms. Environ. Microbiol. **18**: 4403–4411. doi:10.1111/1462-2920.13372

Stoll, M. H. C., K. Bakker, G. H. Nobbe, and R. R. Haese. 2001. Continuous-flow analysis of dissolved inorganic carbon content in seawater. Anal. Chem. **73**: 4111–4116. doi:10.1021/ac010303r

Tammilehto, A., P. C. Watts, and N. Lundholm. 2016. Isolation by time during an Arctic phytoplankton spring bloom. J. Eukaryot. Microbiol. **64**: 248–256. doi:10.1111/jeu.12356

Tatters, A. O., and others. 2013. Short- and long-term conditioning of a temperate marine diatom community to acidification and warming. Philos. Trans. R. Soc. Lond. B Biol. Sci. **368**: 20120437. doi:10.1098/rstb.2012.0437

Thoisen, C., K. Riisgaard, N. Lundholm, T. G. Nielsen, and P. J. Hansen. 2015. Effect of acidification on an Arctic phytoplankton community from Disko Bay, West Greenland. Mar. Ecol. Prog. Ser. **520**: 21–34. doi:10.3354/meps11123

Thomas, M. K., C. T. Kremer, C. A. Klausmeier, and E. Litchman. 2012. A global pattern of thermal adaptation in marine phytoplankton. Science **338**: 1085–1088. doi:10.1126/science.1224836

Tjoelker, M. G., J. Oleksyn, and P. B. Reich. 2001. Modelling respiration of vegetation: Evidence for a general temperature-dependent Q10. Glob. Chang. Biol. **7**: 223–230. doi:10.1046/j.1365-2486.2001.00397.x

Torstensson, A., M. Chierici, and A. Wulff. 2011. The influence of increased temperature and carbon dioxide levels on the benthic/sea ice diatom Navicula directa. Polar Biol. **35**: 205–214. doi:10.1007/s00300-011-1056-4

Tortell, P. D., and others. 2008. CO_2 sensitivity of Southern Ocean phytoplankton. Geophys. Res. Lett. **35**: L04605. doi:10.1029/2007GL032583

Trimborn, S., T. Brenneis, E. Sweet, and B. Rost. 2013. Sensitivity of Antarctic phytoplankton species to ocean acidification: Growth, carbon acquisition, and species interaction. Limnol. Oceanogr. **58**: 997–1007. doi:10.4319/lo.2013.58.3.0997

Valladares, F., and others. 2014. The effects of phenotypic plasticity and local adaptation on forecasts of species range shifts under climate change. Ecol. Lett. **17**: 1351–1364. doi:10.1111/ele.12348

Wadhams, P. 2012. Arctic ice cover, ice thickness and tipping points. Ambio **41**: 23–33. doi:10.1007/s13280-011-0222-9

Conflict of Interest

None declared.